Environmental Science & Technology

Article

pubs.acs.org/est

Reducing Capacities and Distribution of Redox-Active Functional Groups in Low Molecular Weight Fractions of Humic Acids

Zhen Yang,[†] Andreas Kappler,[‡] and Jie Jiang*[,†]

[†]College of Environmental Science and Engineering, Beijing Forestry University, Beijing 100083, China

[‡]Geomicrobiology Group, Center for Applied Geosciences, University of Tüebingen, 72074 Tüebingen, Germany

Supporting Information

ABSTRACT: Humic substances (HS) are redox-active organic compounds with a broad spectrum of molecular sizes and reducing capacities, that is, number of electrons donated or accepted. However, it is unknown which role the distribution of redox-active functional groups in different molecule sizes plays for HS redox reactions in varying pore sizes microenvironments. We used dialysis experiments to separate bulk humic acids (HA) into low molecular weight fractions (LMWF) and retentate, for example, the remaining HA in the dialysis bag. LMWF accounted for only 2% of the total organic carbon content of the HA. However, their reducing capacities per gram of carbon were up to 33 times greater than either those of the bulk HA or the retentate. For a structural/mechanistic understanding of the high reducing capacity of the LMWF, we used fluorescence spectroscopy. We found that the LWMF showed significant fluorescence intensities for quinone-like functional groups, as indicated by the quinoid $\pi-\pi^*$ transition, that are probably responsible for the high reducing capacities. Therefore, the small-sized HS fraction can play a major role for redox transformation of metals or pollutants trapped in soil micropores (<2.5 nm diameter).

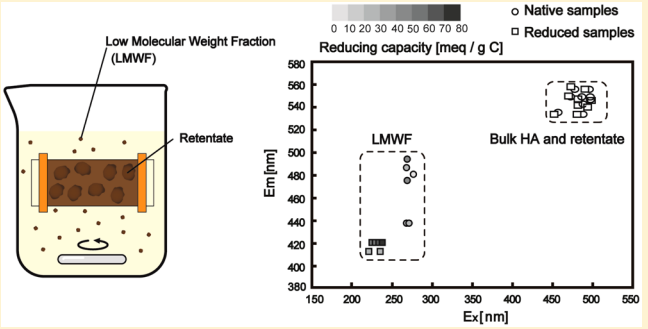

INTRODUCTION

Humic substances (HS) represent a main fraction of soil organic matter and are responsible for many chemical reactions in soil.[1] A variety of organic compounds (e.g., azo dyes, polyhalogenated compounds and nitro-substituted aromatic compounds) and inorganic pollutants (e.g., As(III), Fe(III), C(VI), and U(VI)) are located in soil micropores (<2.5 nm) which limits their uptake by microbes and which is responsible for their recalcitrance.[2−6] The toxicity and mobility of many elements and compounds associated with Fe(III) (oxyhydr)oxide minerals (e.g., arsenic (As), phosphate, etc.) are directly affected by electron transfer reactions between HS and the Fe(III) minerals which can lead to reduction, transformation and dissolution of the Fe minerals.[7−9] Many studies have provided evidence that HS can be reduced both chemically and microbially,[9−11] and that reduced HS have a higher reducing capacity than native ones.[11] Through their redox activity, HS influence biogeochemical processes in anoxic environments and in particular the environmental behavior of metal oxides and organic compounds.[2−5]

HS contain various types of functional groups and the reducing capacities of HS depend on the number of redox-active functional groups and their redox potentials.[3,10,13] Amino compounds participate in self-condensation reactions of quinones during the formation progress of humus[1,14] with quinone moieties considered to be the most important electron-accepting groups for the redox activity of HS.[15] Fluorescence spectroscopy is typically used to characterize and distinguish the fluorophore structure of dissolved organic matter, including humic-like fluorophores and protein-like fluorophores.[16−20] Quinone moieties are traditionally considered as the most important redox-active functional groups in HS, and the fluorescent structure changes of quinone-like compounds and hydroquinones compounds are able to account for the humic-like redox fluorophore characteristics of HS[20−22] before and after reduction. Protein-like fluorophores consist of two different structures that show fluorescence, that is, tyrosine-like and tryptophan-like fluorophores.[23,24] A recent study indicated that absorption bands in the range of 250−300 nm and 330−400 nm in quinone-like fluorophores are related to the quinonoid and benzenoid $\pi-\pi^*$ transition.[21] Reduced quinone fluorophores have a higher intensity of the $\pi-\pi^*$ transition than native quinone fluorophores in the visible region.[21,25]

Until recently, it was commonly assumed that HS are polymeric complex molecules[26] with molecular weights widely ranging from a few hundred up to several million Daltons (Da).[1] However, new research on the molecular structures of HS has shown that HS are supramolecular associations[27−29] of self-assembled, relatively small heterogeneous molecules linked

Received: May 26, 2016
Revised: October 19, 2016
Accepted: October 19, 2016
Published: October 19, 2016

DOI: 10.1021/acs.est.6b02645
Environ. Sci. Technol. 2016, 50, 12105−12113

through hydrogen bridges and hydrophobic bonds instead of the previously assumed tight coiling in the polymer model. Low molecular weight components in Suwannee River fulvic acids (SRFA) have been characterized by using a novel membrane dialysis method.[30] This study confirmed that low molecular weight components in the SRFA, present either individually or in loosely bound assemblies, have a more aliphatic composition relative to bulk SRFA solutions. Although the reactivity of the low molecular weight fraction (LMWF) of HS is expected to be relevant for many biogeochemical processes in the environment, in particular for access to the compounds present in soil micropores, the reducing capacities of the LMWF of HS compared to the bulk HS fraction are unknown.

To simulate the releasing process of the HS LMWF through a soil environment with a variety of micro- and nanopores, we carried out dialysis experiments in order to separate different molecular weight fractions from the bulk HS. The appropriate dialysis membrane pore sizes were chosen due to their relevance for the soil pore sizes where it has been suggested that both 3500 Da molecules and 14 000 Da molecules, with a diameter of 1.25 and 2.5 nm respectively, could flow into and/or out of the micropores.[31] This study first aims to determine the reducing capacities of the different molecular weight fractions of HA. To this end, the LMWF was collected using both 3500 Da and 14 000 Da membrane dialysis and a selection of International Humic Substances Society (IHSS) standard humic acids (HA), that is, Pahokee Peat humic acids (PPHA), Elliott Soil humic acids (ESHA), and Leonardite humic acids (LHA). The second aim of the study was to characterize the redox-active functional groups of the LMWF, the bulk HA and the retentate of HA, using three-dimensional excitation−emission matrix (3DEEM) fluorescence spectroscopy in order to examine the redox-active functional groups distribution of the different molecular weight fractions.

MATERIALS AND METHODS

Source and Preparation of HS. PPHA, ESHA, and LHA were purchased from the IHSS. All HA samples were dissolved in a phosphate buffer solution (PP buffer; 50 mM, pH 7) at a concentration of 0.5 mg/mL. The total organic carbon (TOC) contents of the HA samples were determined by TOC-Vcsn analyzer (SHIMADZU).

Dialysis Experiments. MD34−3500 (pore size 1.25 nm) and MD34−14 000 (pore size 2.5 nm) dialysis bags were chosen to simulate the size of soil micropores.[32] Dialysis bags (MD34−3500, MD34−14 000) from MWCO Regenerate (VISKASE, U.S.) were soaked in deionized water for 24 h before experiments. The dialysis bags containing bulk HA were entirely submerged in a 500 mL PP buffer and the whole device was wrapped in aluminum foil to prevent photochemical reactions. The stirring rate was set to 400 rpm. LMWF was released into the PP buffer, and the retentate remained in the dialysis bags. After 72 h, the retentates in the bags were collected. Samples of LMWF were collected every 24 h.

Determination of the Redox Capacities of HA. HA were chemically reduced by H_2 in the presence of a Pd catalyst (palladium-coated alumina pellets, 0.5% Pd, Merck) and the redox capacities of native (nonreduced) and reduced HA were determined as previously reported by Benz et al.[33] and Kappler et al.[34]

3DEEM. Fluorescence-active functional groups of HA were characterized by the excitation/emission (Ex/Em) wavelengths and fluorescence intensity.[20] The fluorescence spectra of HA were measured in a standard 10 mm quartz cell using a spectrofluorometer (F7000) equipped with 1500 W Xe lamp (Ushio Inc. Japan). 3DEEM were generated at 23 ± 2 °C and at excitation (Ex) and emission (Em) slit intervals of 5.0 nm in each band-pass. Bulk HA and retentate fluorescence spectra were collected under an Ex range from 300 to 500 at 5 nm intervals and an Em range from 400 to 600 at 5 nm intervals. LMWF fluorescence spectra were collected under an Ex range from 200 to 400 at 5 nm intervals and an Em range from 220 to 600 at 5 nm intervals. Ex and Em were then corrected using the PP buffer sample 3DEEM. Intensities were normalized to the area under the PP buffer to obtain relative fluorescence intensities. All HA samples were diluted with a PP buffer to avoid pH changes. The total organic carbon (TOC) contents of all diluted solutions were determined by TOC-Vcsn analyzer (SHIMADZU). 3DEEM of diluted bulk HA with the same TOC content as the LMWF solution were compared to those of the LMWF to exclude concentration effects.[35]

Control Experiments. Control experiments were carried out using pure PP buffer (45 mL) instead of bulk HA solutions in the dialysis bags. Dialysate from the dialysis bags was collected every 24 h and analyzed to determine the potential contribution of organic compounds released from the dialysis bags (Figure S1). Dialysate and PP buffer retentate were then reacted with ferricyanide to determine their reducing capacities (Figure S2). The 3DEEM fluorescence spectra for the PP buffer, PP buffer retentate and dialysate solution are shown in Figure S3.

RESULTS AND DISCUSSION

Dialysis Process and Redox Properties of the LMWF of HA. Dialysis experiments were conducted to separate the different molecular weight fractions of PPHA, ESHA and LHA. The TOC contents for the bulk HA, as well as for the LWMF that was able to pass through pores with a diameter of 1.25 or 2.5 nm (e.g., MW < 3500 Da; MW < 14 000 Da), are listed in Table 1. For all three HA samples, a positive linearity was found for the TOC contents of the LMWF against the dialysis time (Figure 1). The TOC for the different LMWF samples ranged from 4.0 to 4.7 mg C/L. Both the 3500-LMWF and 14 000-LMWF not only showed similar dialysis rates during the dialysis process, but almost the same TOC content of 5 mg C/L at the end of the dialysis process. Constant release rates for the LMWF suggest a continuous disaggregation of the LMWF clusters from the bulk HA. This is consistent with previous studies showing that the molecules of the LMWF either link to the retentate fraction as loosely bound structures[30] or link to each other by hydrogen bonds and hydrophobic interactions.[27]

Table 1. TOC of bulk PPHA, ESHA, and LHA Solutions/Suspensions and Percentage of Two Different Molecular Weight Fractions (in % of the bulk HA TOC)

HA samples	TOC of bulk HA [mg C/L]	14 000-LMWF/Bulk [%]	3500-LMWF/Bulk [%]
PPHA	215.0	2.2	1.9
ESHA	196.4	2.2	2.1
LHA	229.3	1.8	1.8

To investigate the contribution of the LMWF to the redox properties of the entire HA bulk material, an Fe(III)-complex, that is, ferricyanide, was chosen to react with native and reduced LMWF to determine their reducing capacities, that is, the number of electrons that can be transferred from the HS[11,34] to

DOI: 10.1021/acs.est.6b02645
Environ. Sci. Technol. 2016, 50, 12105−12113

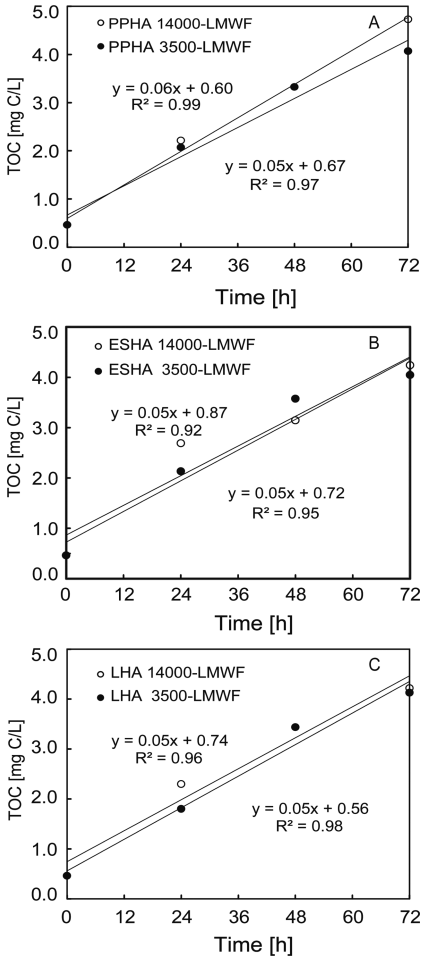

Figure 1. TOC contents of low-molecular weight fractions (LMWF, molecules <3500 Da and <14 000 Da) released over time from bulk HA suspensions ((A) PPHA. (B) ESHA. (C) LHA). Dialysate from dialysis bags was collected every 24 h and analyzed for organic carbon content.

the Fe(III). For all HA samples, significant reducing capacities were measured, i.e. high numbers of electrons transferred from the reduced HA molecules to the Fe (III) complex (Figure 2). This result is consistent with previous studies documenting the redox activities of HS.[3,9,11,12] Most importantly, we were able to show here for the first time that the LMWF in particular exhibits very large reducing capacities. The reducing capacities per liter for bulk PPHA, HA 3500-retentate, and HA 14 000-retentate (Figure 2A) were 0.3 mequiv/L, 0.3 mequiv/L, and 0.3 mequiv/L, respectively. However, considering that the LMWF content accounts for only 2% of the TOC content in the bulk HA molecules, reducing capacities were normalized to the TOC of the HA samples. It was found that the reducing capacities per gram carbon of bulk PPHA, 3500-retentate, and 14 000-retentate were 1.3 mequiv/g C, 1.8 mequiv/g C, and 1.7 mequiv/g C, respectively (Figure 2B). In contrast, the reducing capacities per gram carbon for PPHA 3500-LMWF and PPHA 14 000-LMWF were much higher with values of 42.6 mequiv/g C and 16.8 mequiv/g C, respectively (Figure 2B). This shows that the LMWF reducing capacities of PPHA were approximately 13−33 times higher than that of bulk PPHA and the retentate. Figure 2D and 2F show that the reducing capacities per gram carbon of ESHA and LHA in both the 3500-LMWF and 14 000-LMWF were also far higher than that of the bulk HA and the retentate, similar to PPHA. These results demonstrate that LMWF of HA in particular has a significant reducing capacity, implying that a large number of redox-active functional groups exists in the LMWF, possibly of different types.

The electron accepting capacity is defined as the difference in reducing capacities between reduced and native HA samples. The electron accepting capacity of quinone moieties is 28 mequiv/g C when quinone moieties are reduced and then turn into hydroquinones. The LMWF studied here were shown to have significant electron accepting capacity values ranging from 0.6 to 28.9 mequiv/g C relative to bulk HA with values ranging from 0.9 to 2.5 mequiv/g C (Table 2). With an assumption that quinone moieties are the only/main redox-active functional groups in these HA and all of these quinone moieties can be reduced, we can calculate that the quinone contents (quinone C/g C) of 14000-LMWF (<2.5 nm diameter) range from 27.1 to 103.1%. This is significantly higher than that of bulk HA which ranges from 3.3 to 9.1%. However, it has to be considered that this calculation slightly overestimates the quinone content because there could also be other nonquinone redox-active functional groups present, e.g. redox-active amide groups or redox-active metal ions.[36] Compared with native 3500-LMWF, the reduced 3500-LMWF showed no obvious increase in reducing capacities suggesting that no more redox-active functional groups in the 3500-LMWF could be additionally reduced by H_2. However, reduced 14 000-LMWF exhibited an obvious increase in reducing capacities compared to native 14 000-LMWF. This suggests that the number and chemical identity of redox active functional groups of the molecules in the LMWF are heterogeneously distributed.

Redox Properties of Bulk HA and Retentate. For all three types of bulk HA and retentate, reduced HA were found to have higher reducing capacities than native HA (Figure 2). This result is also in accordance with previous studies describing the redox properties of HS.[11] Notably, the reducing capacities of the retentate were closer to those of the bulk HA, while LMWF showed a higher reducing capacity per gram carbon than the bulk HA. This finding clearly indicates that the distribution of the types and the number of redox-active functional groups in the bulk HA and in the LMWF of the HA varies. The slow release of the LMWF from the bulk HA fraction during dialysis does not influence the number and/or the identity of redox-active functional groups in the retentate HA, suggesting that the reducing capacities of bulk HA and retentate are similar.

At the end of the dialysis experiment two different fractions of HA, one with 45 mL of retentate in the dialysis bags and one with 500 mL of LMWF dialysis solution, were remaining. In order to verify whether the sum of the reducing capacities of the individual fractions balances the value of the reducing capacity of the bulk HA, we calculated the total reducing capacities (TRC, in meq) of each fraction, by multiplying the values for the reducing capacity (meq/L) times the volume (L), to obtain a total electron balance (Figure 3). For all three HA samples, the TRC for the 3500-LMWF was nearly ten times higher than that of the 3500-retentate. The TRC of the bulk HA was nearly the same as the TRC for the retentate. Furthermore, we calculated that the sum of the $TRC_{retentate}$ and TRC_{LMWF} was more than two or six times higher than the $TRC_{bulk\ HA}$.

These results suggest that after the release of the LMWF from the bulk HA fraction, the retentate HA showed similar redox properties (e.g., reducing capacity and electron accepting capacity)

DOI: 10.1021/acs.est.6b02645
Environ. Sci. Technol. 2016, 50, 12105−12113

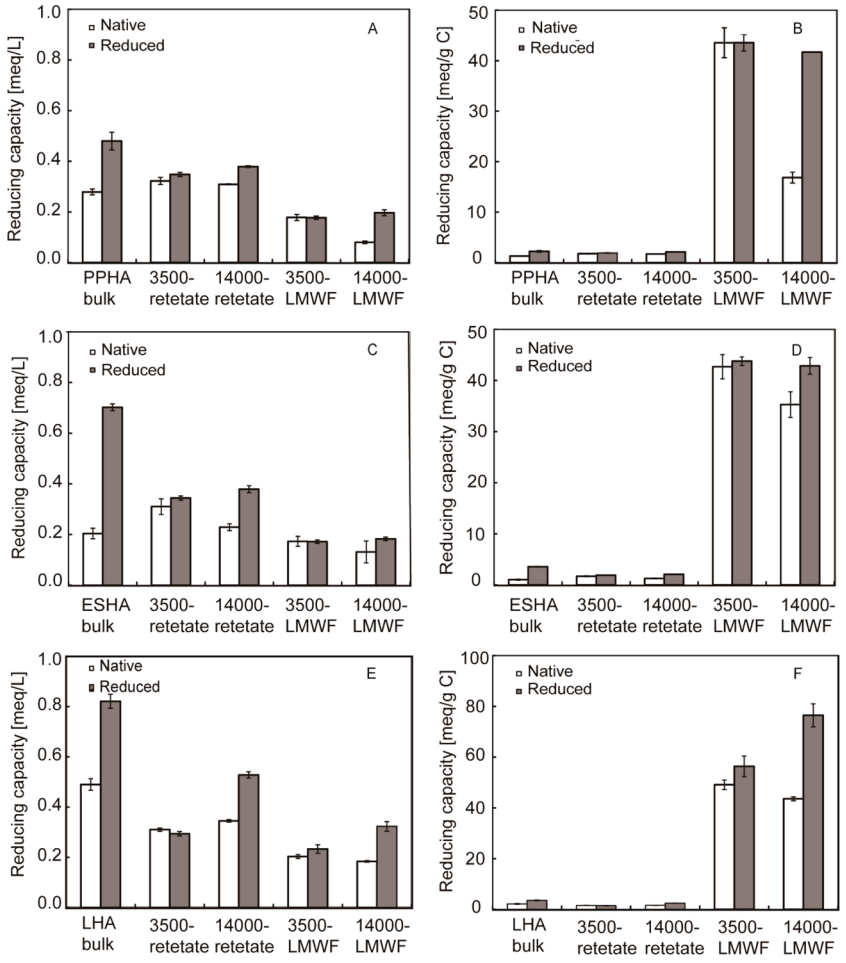

Figure 2. Comparison of reducing capacities of different molecular weight fractions of HA in their native and reduced state. Reduced HA were prepared by chemical reduction by H_2 in the presence of a Pd catalyst. Native and reduced HA samples reacted with ferricyanide to determine their reducing capacity. The error bars represent the standard deviation of three independent reactors. (A) (C) (E) Reducing capacities per liter volume of native and reduced bulk HA, retentate and LWMF of PPHA ESHA and LHA. (B) (D) (F) Reducing capacities per gram carbon, normalized to TOC contents of HA fractions, of native and reduced bulk HA, retentate and LWMF of PPHA ESHA and LHA.

Table 2. Quinone Content of HA and Low Molecular Weight Fractions of HA Calculated from Their Electron Accepting Capacities

HA samples		electron accepting capacities (meq/g C)	quinone contents (quinone C/g C) in (%)
PPHA	bulk HA	0.93	3.3
	3500-LMWF	0.64	2.3
	14 000-LMWF	24.87	88.8
ESHA	bulk HA	2.54	9.1
	3500-LMWF	1.24	4.4
	14 000-LMWF	7.59	27.1
LHA	bulk HA	1.44	5.1
	3500-LMWF	12.26	43.8
	14 000-LMWF	28.86	103.1

as the bulk HA. Therefore, the retentate and bulk HA probably possess a comparable number and distribution of redox-active functional groups. However, it also suggests that the LMWF undergoes a major structural/conformational change[28] during separation from the bulk HA and that these changes lead to a significant increase in redox-activity probably by new exposure

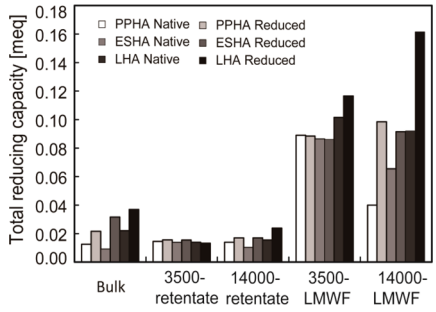

Figure 3. Total reducing capacity (TRC, meq) calculated for bulk HA, retentate and LMWF of PPHA, ESHA, and LHA in their native and reduced redox state.

of previously inaccessible redox-active functional groups, i.e. these functional groups are then accessible for electron transfer to Fe(III).

Characteristic Fluorescence Properties of LMWF of HA samples. Fluorescence spectroscopy is typically used to characterize and distinguish the fluorophore structure. The typical fluorophores in HS include humic-like fluorophores and protein-like fluorophores. Characteristic fluorescence properties, including excitation wavelength/emission wavelength data and

DOI: 10.1021/acs.est.6b02645
Environ. Sci. Technol. 2016, 50, 12105−12113

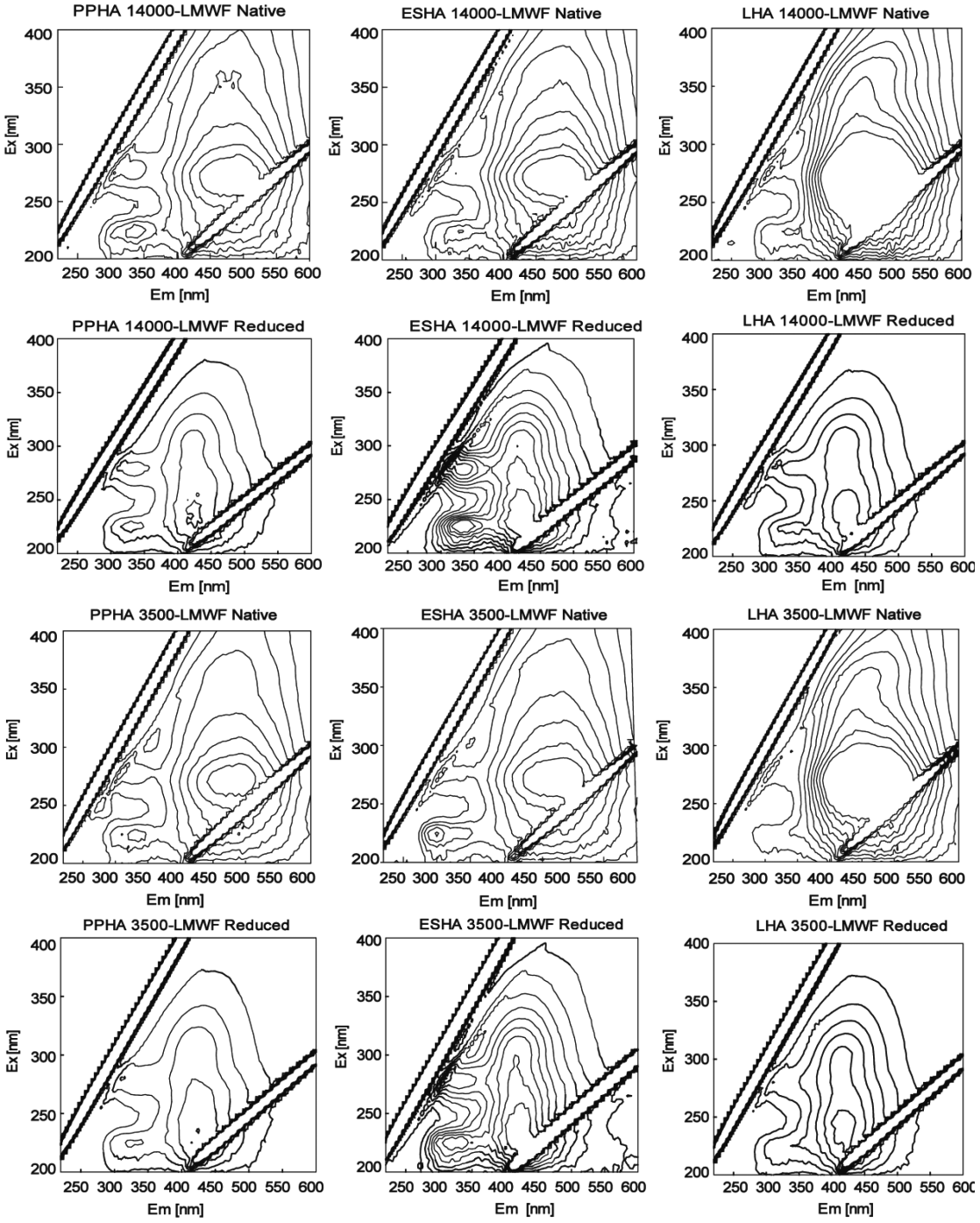

Figure 4. 3DEEM fluorescence spectra of different LMWF of PPHA, ESHA, and LHA in their native and reduced redox state. Ex and Em represent the excitation and emission wavelengths, respectively, indicating the main fluorophore peak positions.

fluorescence intensity of LMWF, for the retentate and bulk HA were detected using 3DEEM in order to determine the distribution of redox-active functional groups. Quinone moieties are considered as the most important redox-active functional groups in HS. The fluorescent structure characteristics of quinone-like compounds and hydroquinone-like compounds are responsible for the humic-like fluorophore characteristics of HS[20−22] in native and reduced state, respectively. Reducing capacities of the different molecular weight fractions of HA are related to the characteristics of quinone-like/hydroquinone-like fluorophores and they in particular to explain the significant difference in reducing capacity of the LMWF of the HA compared to bulk HA and retentate. The characteristic fluorescence spectra for LMWF of PPHA, ESHA, and LHA are shown in Figure 4 and fluorescence peak positions and relative fluorescence intensities are listed in Table 3. LMWF fluorescence spectra showed two distinct types of fluorescence groups including humic-like fluorophores (Em > 400 nm) and protein-like fluorophores.[17,19] The protein-like fluorophores had a tryptophan-like peak (Ex 270−280 or <240 nm; Em 330−368 nm) and a tyrosine-like peak (Ex 270−275 nm; Em 304−312 nm). The fluorescence intensities of LMWF were 5.30−10.54 au for the tryptophan-like peak and 6.50−9.80 au for the tyrosine-like peak. In the control experiment (i.e., only

DOI: 10.1021/acs.est.6b02645
Environ. Sci. Technol. 2016, 50, 12105−12113

Table 3. Fluorescence Peak Positions and Relative Fluorescence Intensities of Different Native and Reduced LMWF of PPHA, ESHA and LHA

	3500- LMWF Native				3500- LMWF Reduced				14000- LMWF Native				14000- LMWF Reduced			
	Ex/Em[a] [nm]	intensity[b] [a.u]	Peak Type	transition section	Ex/Em[a] [nm]	intensity[b] [a.u]*	Peak Type	transition section	Ex/Em[a] [nm]	intensity[b] [a.u]*	Peak Type	transition section	Ex/Em[a] [nm]	iintensity[b] [a.u]*	peak type	transition section
PPHA	220/330	7.92	tryptophan-like		225/315	18.39	tryptophan-like		225/340	10.54	tryptophan-like		225/335	18.78	tryptophan-like	
	275/305	8.46	tyrosine-like		270/300	13.58	tyrosine-like		275/305	9.80	tyrosine-like		280/335	19.04	tryptophan-like	
	270/495	18.00	quinone-like	quinonoid $\pi-\pi^*$	225/415	28.19	quinone-like	benzenoid $\pi-\pi^*$	275/485	19.16	quinone-like	quinonoid $\pi-\pi^*$	230/420	29.45	quinone-like	benzenoid $\pi-\pi^*$
	365/470	7.94	quinone-like	quinonoid $\pi-\pi^*$	300/450	22.15	quinone-like	quinonoid $\pi-\pi^*$	355/465	9.09	quinone-like	quinonoid $\pi-\pi^*$	305/425	24.43	quinone-like	quinonoid $\pi-\pi^*$
ESHA	225/300	11.66	tryptophan-like		225/335	17.98	tryptophan-like		225/340	9.38	tryptophan-like		225/330	25.85	tryptophan-like	
	270/300	7.86	tyrosine-like		270/300	18.44	tyrosine-like		280/310	8.22	tyrosine-like		280/335	22.30	tryptophan-like	
	270/480	18.91	quinone-like	quinonoid $\pi-\pi^*$	235/420	22.84	quinone-like	benzenoid $\pi-\pi^*$	270/490	24.51	quinone-like	quinonoid $\pi-\pi^*$	235/415	22.72	quinone-like	benzenoid $\pi-\pi^*$
	360/485	8.64	quinone-like	quinonoid $\pi-\pi^*$	285/415	18.33	quinone-like	quinonoid $\pi-\pi^*$	345/490	11.83	quinone-like	quinonoid $\pi-\pi^*$	300/415	18.00	quinone-like	quinonoid $\pi-\pi^*$
LHA	225/305	4.30	tryptophan-like		220/315	14.50	tryptophan-like		225/335	7.61	tryptophan-like		225/335	20.43	tryptophan-like	
	275/305	6.50	tyrosine-like		275/305	17.27	tyrosine-like		280/315	8.55	tyrosine-like		280/340	18.80	tryptophan-like	
	270/450	32.67	quinone-like	quinonoid $\pi-\pi^*$	240/420	36.63	quinone-like	benzenoid $\pi-\pi^*$	270/450	35.53	quinone-like	quinonoid $\pi-\pi^*$	245/420	31.77	quinone-like	benzenoid $\pi-\pi^*$
	345/445	14.87	quinone-like	quinonoid $\pi-\pi^*$	295/415	30.35	quinone-like	quinonoid $\pi-\pi^*$	345/445	16.49	quinone-like	quinonoid $\pi-\pi^*$	300/415	26.33	quinone-like	quinonoid $\pi-\pi^*$

[a]Ex/Em represents the excitation/emission, which indicating the main fluorophores peaks position° b. 355 nm. [b]The fluorescence intensities refer to the relative fluorescence intensities. Intensities were normalized to the area under the peak (Ex) at 355 nm determined in PP buffer (50 mM, pH 7).

DOI: 10.1021/acs.est.6b02645
Environ. Sci. Technol. 2016, 50, 12105−12113

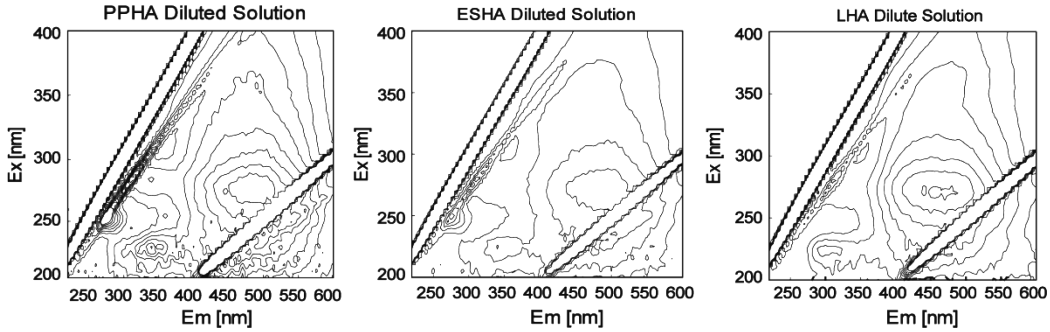

Figure 5. 3DEEM fluorescence spectra of diluted PPHA, diluted ESHA and diluted LHA. The diluted HA (TOC = 4.2 mg C/L) have the same TOC contents as the HA LMWF.

PP buffer in the dialysis bags without HA), neither protein-like fluorophores nor humic-like fluorophores were be detected (Figure S3) demonstrating that protein-like fluorescence peaks resulted from the LMWF and not from dialysis bag impurities.

The humic-like fluorophore (Em > 400 nm) properties are related to quinone-like fluorophores, which have absorption wavelengths (Ex wavelengths) at 250−300 nm and 330−400 nm due to quinone and benzenoid $\pi-\pi^*$ transitions.[21] Quinone-like moieties are generally considered as the main redox-active functional groups of HS and the distribution of quinone-like fluorophores contribute to the gradients of oxidized and reduced functional groups within the HS molecules. The peak positions (Ex/Em) of quinone-like fluorophores for all LMWF HA samples were located at 270−275/450−495 nm and 345−365/445−490 nm due to quinone $\pi-\pi^*$ transitions, and fluorescence intensities of quinone-like fluorophores ranged between 18.0 and 35.53 au and 7.94−16.69 au. The number of quinone-like fluorophores was greater than the number of protein-like fluorophores for LMWF HA (Figure S4), that is, LHA 3500-LMWF, and the fluorescence intensities of the quinone-like and protein-like fluorophore are 47.54 au and 10.8 au, respectively. This result implies that quinone-like fluorophores dominate the main fluorophore type of LMWF, which accounts for the higher reducing capacities of LMWF HA than that of bulk HA and retentate.

After reduction, taking LHA as example, the Ex/Em peak positions of tryptophan-like and tyrosine-like fluorophores were located at 220/315 nm and 275/305 nm for LHA 3500-LMWF reduced, and 225/335 nm and 280/340 nm for LHA 14 000-LMWF reduced (Table 3). Ex/Em positions for the reduced quinone-like fluorophores were located at 240/420 nm due to benzenoid $\pi-\pi^*$ transitions and at 295/415 nm due to quinone $\pi-\pi^*$ transitions for LHA 3500-LMWF. For LHA 14 000-LMWF, these Ex/Em peaks were located at 245/420 nm due to benzenoid $\pi-\pi^*$ transitions and 300/415 nm due to quinone $\pi-\pi^*$ transitions. For all reduced LMWF HA samples, compared to the native LMWF HA, the fluorescence intensity increased for both the reduced protein-like and reduced quinone-like fluorophores, which indicates that the number of redox-active functional groups increased. Moreover, the peak positions of the reduced quinone-like fluorophores shifted to significantly shorter wavelengths to 65 nm for Ex wavelengths and 80 nm for Em wavelengths. The reduction of protein-like fluorophore also resulted in peaks shifting to shorter wavelengths, by 5 nm for both Ex and Em wavelengths. These results suggest that the quinone-like groups are responsible for the redox reactions of LMWF, and produce small levels of conjugated chromophores in the quinone-like groups.[20]

Relative to 3500-LMWF, the 14 000-LMWF had a higher fluorescence intensity for the quinone-like fluorophores. This means that, compared to the 3500-LMWF, the number of quinone-like groups of 14 000-LMWF is higher, indicating a more intense π electron system of the quinone-like groups for the 14 000-LMWF. The quinone contents of 14 000-LMWF (27−103% quinone C/g C) are higher than those of 3500-LMWF (2.3−43.8% quinone C/g C). More quinone-like groups and a more complex π-electron-system for 14 000-LMWF relative to 3500-LMWF has contributed to the high electron accepting capacity of the LMWF (Table 2).

Additionally, in order to show that the dilution of HA solutions does not lead to conformational/structural changes of HA and thus higher amounts of redox fluorophores and a higher reducing capacity, the fluorescence data is shown in Figure 5 and Table 3 for diluted bulk PPHA, ESHA, and LHA, all with the same TOC content as the analyzed LMWF. Relative to the dialyzed LMWF HA samples, the fluorescence intensities (both protein and quinone-fluorophores) of the diluted HA samples were lower and the fluorescence peak positions of the LMWF HA samples showed a red shift, i.e. a shift to longer wavelengths (Table 4). Furthermore, LMWF HA had a 2−4 times higher per gram carbon reducing capacity relative to the diluted HA samples (Figure S6). These results suggest that simply diluting HA solutions does not explain the higher reducing capacities observed in the LMWF that was separated from the bulk HA by dialysis.

Table 4. Fluorescence Parameters of Diluted HA (TOC 4.2 mg C/L)

	Ex/Em[a] [nm]	Intensity[b] [a.u]	peak type
PPHA	225/340	4.02	tryptophan-like
	275/485	4.96	quinone-like
	280/310	5.41	other types
ESHA	225/340	2.99	tryptophan-like
	270/490	5.31	quinone-like
	310/350	2.97	other types
LHA	225/335	3.96	tryptophan-like
	270/450	8.32	quinone-like
	315/355	2.72	other types

[a]Ex/Em represents the excitation/emission, which indicating the main fluorophore peak positions. [b]The fluorescence intensities refer to the relative fluorescence intensities. Intensities were normalized to the area under the peak (Ex) at 355 nm determined in PP buffer (50 mM, pH 7).

DOI: 10.1021/acs.est.6b02645
Environ. Sci. Technol. 2016, 50, 12105−12113

Characteristic Fluorescence Properties of bulk and retentate HA. The characteristic fluorescence spectra for all bulk HA and retentate were in the range of Ex 480−490/Em 545−560 nm, and relative fluorescence intensities range from 0.64 au to 3.03 au (Figure S4, Table S1). The fluorescence spectra of bulk HA were very similar to those of the retentate, both with regard to fluorescence peak position and relative fluorescence intensities. For example, we determined Ex/Em peaks at 490/554 nm for the bulk PPHA and 485/555 nm for PPHA 14 000-retentate and 485/555 nm for PPHA 3500-retentate as well as relative fluorescence intensities of 0.77, 0.69, and 0.68 au for this excitation/emission peak for the three fractions, respectively.

We also observed a characteristic change of fluorescence spectra during reduction that was similar between retentate and initial HA. For reduced bulk PPHA, PPHA 14 000-retentate and PPHA 3500-retentate the Ex/Em peak positions were located at 480/550 nm, 480/550 nm and 480/555 nm, respectively, and the relative fluorescence intensities were 0.61 au, 0.54 au, and 0.51 au, respectively. Compared with native bulk PPHA, PPHA 14 000-retentate and PPHA 3500-retentate, peak positions for all reduced samples showed a blue shift, that is, a shift to shorter wavelengths, of the peak positions by 5−10 nm for the excitation wavelength and 5 nm for the emission wavelength. The decrease in fluorescence intensity and the blue shift of the fluorescence peak positions after reduction for bulk and retentate HA corresponded to a significant increase in reducing capacities after reduction. The characteristic fluorescence changes during reduction indicate that reduced HA samples have an increased π-electron system relative to native bulk and retentate. These results demonstrated compared with the native state, a lower degree of conjugated system effect within the (aromatic ring) structures[20] for reduced bulk HA and retentate. The reason for this is probably that during the reduction, some double bonds of conjugated structures become reduced to single bonds. These single bonds interrupt the conjugation thus explaining why we see a decreasing number of conjugated bonds in the reduced state of the HA molecules structure.[36]

In Figure 6, the relationship between the reducing capacity and the fluorophore positions is shown. The quinone-like fluorophores were found to be the main contributing moieties of fluorophores to the reducing capacities of the LMWF. Relative to the bulk HA and retentate, the LMWF owes their high reducing capacity to shorter Ex/Em wavelengths. Furthermore, the Ex/Em positions of reduced LMWF shift to shorter wavelengths correlating with an increased reducing capacity compared to native LMWF. Such a release of LMWF is probably of particular relevance in fresh humic substances as they are present in wetlands or biologically/microbially active sediments and groundwater aquifers with fresh organic matter input and/or production.

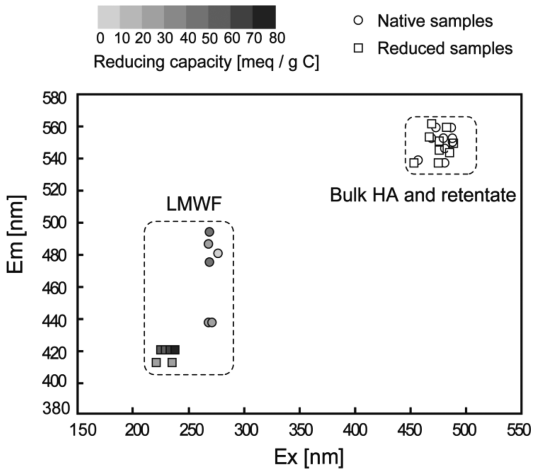

Figure 6. Relationship between reducing capacities and fluorescence peak positions (Ex/Em) for different molecular weight fractions of PPHA, ESHA and LHA (the darker the gray scale of the symbols, the higher the reducing capacity). Quinone-like fluorophores are considered as the main contributing moieties to the reducing capacities of the LMWF.

Environmental Implications. In porous geological media (soils, sediments and aquifer materials) nanoscale pores account for over 90% of the total mineral surface area,[37] and micropores (<2 nm) in soil account for 10% of the macropore volume of soil.[31] It has been debated whether mineral and organic compounds hidden in soil micropores, inhibiting their uptake by microbes and enhancing their recalcitrance, can be transformed or degraded. Based on the results shown here, it seems likely that LMWF—both 3500 Da molecules and 14 000 Da molecules with only 1.25 and 2.5 nm diameters, respectively—could flow into and/or out of the micropores. We found that the distribution of redox-active functional groups is different for small and large HA molecules, with a much higher number of quinone-like fluorophores present in small molecules. This suggests that in particular the small HA molecules can significantly influence the electron transfer to Fe compounds and other redox reactions in soil. Based on our data the bulk HA fraction can function as a stock for small HA molecules that can be released under appropriate environment conditions (e.g., by traveling through soil micropores).

Furthermore, the development of a relationship between the reducing capacity and the fluorescence peak positions as shown here (Figure 6) offers a simple alternative to complex chemical analyses, to predict the relative reducing capacities of HS in aqueous environments, based simply on the Ex/Em positions.

■ ASSOCIATED CONTENT

Ⓢ Supporting Information

The Supporting Information is available free of charge on the ACS Publications website at DOI: 10.1021/acs.est.6b02645.

PP buffer dialysate was collected every 24 h to eliminate the disturbance produced from dialysis bags (Figure S1). PP buffer dialysate and retentate in dialysis bags were reacted with ferricyanide to determine the reducing capacities (Figure S2). 3DEEM fluorescence spectra of PP buffer bulk, PP buffer retentate and dialyzed PP buffer are shown in figure S3. Fluorescence information for the bulk HA and retentate is shown in Figure S4 and Table S1. Comparison of the fluorescence intensity of the fluorophores for bulk HA and LMWF are shown in Figure S5. Reducing capacities for PPHA LMWF, and diluted PPHA are shown in Figure S6 (PDF)

■ AUTHOR INFORMATION

Corresponding Author

*Phone: +861062336615; e-mail: jiangjie@bjfu.edu.cn.

Notes

The authors declare no competing financial interest.

■ ACKNOWLEDGMENTS

This research was supported by the National Natural Science Foundation of China (21307004) to J.J.

DOI: 10.1021/acs.est.6b02645
Environ. Sci. Technol. 2016, 50, 12105−12113

REFERENCES

(1) Stevenson, F. J. *Humus Chemistry: Genesis, Composition, Reactions*, 2nd ed.; John Wiley & Sons: New York, 1994.

(2) Curtis, G. P.; Reinhard, M. Reductive dehalogenation of hexachlorethane, carbon- tetrachloride, and bromoform by anthrahydroquinone disulfonate and humic-acid. *Environ. Sci. Technol.* **1994**, *28* (13), 2393−2401.

(3) Kappler, A.; Haderlein, S. B. Natural organic matter as reductant for chlorinated aliphatic pollutants. *Environ. Sci. Technol.* **2003**, *37* (12), 2714−2719.

(4) Gu, B.; Chen, J. Enhanced microbial reduction of Cr(VI) and U(VI) by different natural organic matter fractions. *Geochim. Cosmochim. Acta* **2003**, *67* (19), 3575−3582.

(5) Piepenbrock, A.; Schroeder, C.; Kappler, A. Electron transfer from humic substances to biogenic and abiogenic Fe(III) oxyhydroxide minerals. *Environ. Sci. Technol.* **2014**, *48*, 1656−1664.

(6) Klüpfel, L.; Piepenbrock, A.; Kappler, A.; Sander, M. Humics as fully regenerable terminal electron acceptors in recurrently anoxic environments[J]. *Nat. Geosci.* **2014**, *7*, 195−200.

(7) Melton, E. D.; Swanner, E. D.; Behrens, S.; Schmidt, C.; Kappler, A. The interplay of microbially mediated and abiotic reactions in the biogeochemical Fe cycle. *Nat. Rev. Microbiol.* **2014**, *12*, 797−808.

(8) Piepenbrock, A.; Kappler, A., Humic substances and extracellular electron transfer. In *Metal respiration - from Geochemistry to Potential Applications*; Johannes Gescher, Andreas, Kappler, Eds.; Springer Press: Heidelberg, Germany, 2012.

(9) Borch, T.; Kretzschmar, R.; Kappler, A.; Van Cappellen, P.; Ginder-Vogel, M.; Voegelin, A.; Campbell, K. Biogeochemical Redox Processes and their Impact on Contaminant Dynamics. *Environ. Sci. Technol.* **2010**, *44* (1), 15−23.

(10) Lovley, D. R.; Coates, J. D.; Blunt-Harris, E. L.; Phillips, E. J. P.; Woodward, J. C. Humic substances as electron acceptors for microbial respiration. *Nature* **1996**, *382* (6590), 445−448.

(11) Jiang, J.; Kappler, A. Kinetics of microbial and chemical reduction of humic substances: Implications for electron shuttling. *Environ. Sci. Technol.* **2008**, *42* (10), 3563−3569.

(12) Roden, E.; Kappler, A.; Bauer, I.; Jiang, J.; Paul, A.; Stoesser, R.; Konishi, H.; Xu, H. Microbial reduction of solid-phase humics and electron shuttling to Fe(III) oxide. *Nat. Geosci.* **2010**, *3*, 417−421.

(13) Struyk, Z.; Sposito, G. Redox properties of standard humic acids. *Geoderma* **2001**, *102* (3−4), 329−346.

(14) Enders, C.; Windisch, S. The decomposition of nicotine by yeast. *Biochem* **1947**, *318*, 54−62.

(15) Scott, D. T.; McKnight, D. M.; Blunt-Harris, E. L.; Kolesar, S. E.; Lovley, D. R. Quinone moieties act as electron acceptors in the reduction of humic substances by humics-reducing microorganisms. *Environ. Sci. Technol.* **1998**, *32* (19), 2984−2989.

(16) Coble, P. G.; Green, S. A.; Blough, N. V.; Gagosian, R. B. Characterization of dissolved organic matter in the Black Sea by fluorescence spectroscopy. *Nature* **1990**, *348* (6300), 432−435.

(17) Coble, P. G. Characterization of marine and terrestrial DOM in seawater using excitation-emission matrix spectroscopy. *Mar. Chem.* **1996**, *51* (4), 325−346.

(18) Parlanti, E.; Wörz, K.; Geoffroy, L.; Lamotte, M. Dissolved organic matter fluorescence spectroscopy as a tool to estimate biological activity in a coastal zone submitted to anthropogenic inputs. *Org. Geochem.* **2000**, *31* (12), 1765−1781.

(19) Fellman, J. B.; Hood, E.; Spencer, R. G. M. Fluorescence spectroscopy opens new windows into dissolved organic matter dynamics in freshwater ecosystems: A review. *Limnol. Oceanogr.* **2010**, *55* (6), 2452−2462.

(20) Senesi, N.; D'Orazio, V., Fluorescence spectroscopy. In *Encyclopedia of Soils in the Environment*; Hillel, D., Ed.; Elsevier Press: Oxford, 2005; pp 35−52.

(21) Cory, R. M.; McKnight, D. M. Fluorescence spectroscopy reveals ubiquitous presence of oxidized and reduced quinones in dissolved organic matter. *Environ. Sci. Technol.* **2005**, *39* (21), 8142−8149.

(22) Fellman, J. B.; Miller, M. P.; Cory, R. M.; D'Amore, D. V.; White, D. Characterizing Dissolved Organic Matter Using PARAFAC Modeling of Fluorescence Spectroscopy: A Comparison of Two Models. *Environ. Sci. Technol.* **2009**, *43* (16), 6228−6234.

(23) Yamashita, Y.; Tanoue, E. Chemical characterization of protein-like fluorophores in DOM in relation to aromatic amino acids. *Mar. Chem.* **2003**, *82* (3−4), 255−271.

(24) Maie, N.; Scully, N. M.; Pisani, O.; Jaffé, R. Composition of a protein-like fluorophore of dissolved organic matter in coastal wetland and estuarine ecosystems. *Water Res.* **2007**, *41* (3), 563−570.

(25) Babaei, A.; Connor, P. A.; McQuillan, A. J.; Umapathy, S. UV-Visible Spectrooelectrochemistry of the Reduction Products of Anthraquinone in Dimethylformamide Solutions: An Advanced Undergraduate Experiment. *J. Chem. Educ.* **1997**, *74* (10), 1200.

(26) Khan, S. U.; Schnitze, M. Permanganate oxidation of humic acids, fulvic acids, and humins extracted from ah horizons of a black chernozem, a black solod, and a black solonetz soil. *Can. J. Soil Sci.* **1972**, *52* (1), 43−51.

(27) Piccolo, A. The supramolecular structure of humic substances. *Soil Sci.* **2001**, *166* (11), 810−832.

(28) Lehmann, J.; Kleber, M. The contentious nature of soil organic matter.[J]. *Nature* **2015**, *528* (7580), 60−68.

(29) Sutton, R.; Sposito, G. Molecular structure in soil humic substances: The new view. *Environ. Sci. Technol.* **2005**, *39* (23), 9009−9015.

(30) Remucal, C. K.; Cory, R. M.; Sander, M.; McNeill, K. Low molecular weight components in an aquatic humic substance as characterized by membrane dialysis and orbitrap mass spectrometry. *Environ. Sci. Technol.* **2012**, *46* (17), 9350−9359.

(31) Echeverría, J. C.; Morera, M. T.; Mazkiarán, C.; Garrido, J. J. Characterization of the porous structure of soils: adsorption of nitrogen (77 K) and carbon dioxide (273 K), and mercury porosimetry. *Eur. J. Soil Sci.* **1999**, *50* (3), 497−503.

(32) Sing, K. S. W.; Everett, D. H.; Haul, R. A. W.; Moscou, L.; Pierotti, R. A.; RouqueÂrol, J.; Siemieniewska, T. Reporting physisorption data for gas/solid systems with special reference to the determination of surface-area and porosity. *Pure Appl. Chem.* **1985**, *57*, 603−619.

(33) Benz, M.; Schink, B.; Brune, A. Humic acids reduction by propionibacterium freudenreichii and other fermenting bacteria. *Appl. Environ. Microb.* **1998**, *64* (11), 4507−4512.

(34) Kappler, A.; Benz, M.; Schink, B.; Brune, A. Electron shuttling via humic acids in microbial iron(III) reduction in a freshwater sediment. *FEMS Microbiol. Ecol.* **2004**, *47* (1), 85−92.

(35) Mobed, J. J.; Hemmingsen, S. L.; Autry, J. L.; McGown, L. B. Fluorescence characterization of ihss humic substances: total luminescence spectra with absorbance correction. *Environ. Sci. Technol.* **1996**, *30* (10), 3061−3065.

(36) Cohrs, C.; Reuchlein, H.; Musch, P. Experimental Assessment of the Effect of a Bicyclo[1.1.0]butane System in Strain-Induced Localisation of Aromatic π-Bonds[J]. *Eur. J. Org. Chem.* **2003**, *2003* (5), 901−906.

(37) Wang, Y. Nanogeochemistry: Nanostructures, emergent properties and their control on geochemical reactions and mass transfers. *Chem. Geol.* **2014**, *378*−*379* (0), 1−23.

DOI: 10.1021/acs.est.6b02645
Environ. Sci. Technol. 2016, 50, 12105−12113